Effects of Humidity on the Performance of Ionic Polymer−Metal Composite Actuators: Experimental Study of the Back-Relaxation of Actuators

Eiichi Shoji* and Daisuke Hirayama

Department of Human and AI Systems, Intelligent Materials Science and Technology Laboratory, University of Fukui, 3-9-1 Bunkyo, Fukui 910-8507, Japan

Received: June 14, 2007; In Final Form: July 31, 2007

This article focuses on the dependence of water uptake on the displacement, velocity, mechanical force, and charging profiles of perfluorinated ionomer−platinum/Li^+-based actuators. Both the displacement and force generation were found to be strongly dependent on the humidity. The primary reason for this effect is a decrease in the stiffness as a result of the humidity. The actuators demonstrated a dramatic reverse motion and a negative force, and this subsequent relaxation was dramatically decreased by decreasing humidity. This relaxation process can be explained by the slow diffusion of water into the elastically softened anode and out of the stiffened cathode. There are no clear inflection points on the charging profile during the reverse relaxation, and this suggests that the relaxation process does not involve a major redistribution of counter cations. An increase in water uptake resulted in an enhancement of the velocity of the displacement. A continuous generation of force was also examined by scanning potential, and the force was proportional to the potential. Humidities near 50−60% (i.e., water uptakes of ca. 5 wt %) gave a better actuator bending performance.

Introduction

To date, various polymers, such as polymer gels,[1−4] ion-exchange polymers,[5−13] and conducting polymers,[14−17] among others, have attracted attention as active sensors, flexible and lightweight actuators, artificial muscles, and energy transducers. For the past decade, ionic polymer−metal composites (IPMCs) have been extensively studied as new materials. IPMC actuators consist of a host polymer bound by thin metal surfaces, where the two metallic surfaces are conductive. The host polymer usually consists of perfluorinated ionomers such as Nafion (E.I. DuPont de Nemours & Co. Inc.) and Flemion (Asahi Glass Co. Ltd.). Scheme 1 shows the chemical structure of Nafion, where $x = 6.5$, $y = 1$, $z = 1$ corresponds to Nafion 117.[18] The polyelectrolyte matrix was neutralized by the presence of counterions, balancing the charge of the anions covalently fixed to the membrane. This polymer has a unique morphological structure that has a two-phase system of an ion cluster network surrounded by a hydrophobic poly(tetrafluoroethylene) (PTFE) medium,[19] The cluster network contributes a dynamic bending performance to the actuators. In various modeling and experimental works, the phase-separated domains have been revealed to be spherical inverted micellar structures connected by short narrow channels.[20,21] The length of the side chains affects the separation between the ionic and nonpolar domains, and the counterions such as Li^+ or Na^+ are mobile and solvated by water within nanoclusters with sizes of 3−5 nm. Nobel metals such as platinum and gold are usually plated as IPMC electrodes on both sides of the film by an electroless plating method.

IPMC actuators give larger displacements than other chemical actuators, and they are lightweight, noiseless, easy to produce, and generate no EMI (electromagnetic interference). They can be operated at relatively low voltages in the range of 1−3 V and can be used under water and in the air. It is noted that their mechanical characteristics are similar to those of biological muscles in terms of flexibility, softness, and ability to undergo large deformations.[22] These unique features are attractive for potential applications of cutting-edge actuators in artificial muscles, robotic arms, micromanipulators, and micropumps.[23] To understand the actuation mechanism of IPMCs, several feasible numerical and experimental models based on hypotheses and analytical chemical processes have been proposed.[22] For example, a model based on the spatial distribution of the ions in an electric field and a pH gradient,[24] an Euler−Bernoulli beam model,[25] a linear dynamic lumped-parameters model,[26] a black-box model based on a network of a capacitor and resistor,[27] a higher-order lumped-parameter model dealing with the relaxation phenomena,[28] a model based on microstructure of Nafion and a phase separation morphology,[29] a model based on water transport across the membrane dealing with deformation and relaxation phenomena,[30] and a model based on the concentration of water molecules dealing with mass transport and chemical reactions at boundaries have been reported to understand the deformation of the actuators.[22]

SCHEME 1

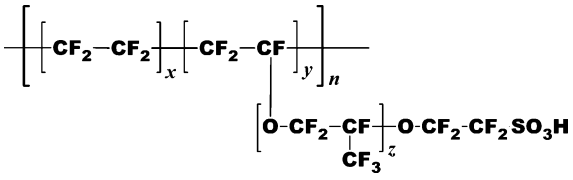

Although these models are well proposed, a detailed mechanism for the generation of the large displacement and back-relaxation phenomena of the actuator is not yet fully elucidated. It seems that the mobility of ion−water clusters and water redistribution affect the deformation and stress relaxation phenomena. Here, understanding water migration under an

* To whom correspondence should be addressed. E-mail: shoji@chem.his.fukui-u.ac.jp.

10.1021/jp074611q CCC: $37.00
Published on Web 09/21/2007

applied electric field is an important subject for IPMC-type actuators. To develop an understanding of actuator performance, more experimental findings regarding the effects of water uptake on the performance of actuators are still needed.

The purpose of the present contribution is to report on such experimental findings and the performance of IPMC-type actuators. In this work, the effects of water migration on the behavior of the displacement were examined by changing the humidity to manipulate the water uptake in the film. Profiles of the displacement, velocity, and force were carefully examined. The stress relaxation process of an actuator film due to water redistribution could be a key subject for understanding the displacement and force processes.

Experimental Section

Materials. Nafion 117 (equiv wt 1100, thickness ca. 180 μm), sodium borohydride (>98% grade), and $[Pt(NH_3)_4]Cl_2$ [tetraamineplatinum(II) chloride, >98%] were purchased from Aldrich and used as received. Nitric acid (concentrated, 70%) and lithium hydroxide monohydrate (>98%) were purchased from Wako Pure Chemical Industries, Ltd. Water (18 MΩ) from a Millipore purification system was used for all experiments unless otherwise noted.

Preparation of the Actuator. The preparation method used herein is based on a reported procedure.[31] The IPMC composite film was carefully washed and soaked in pure water and used as freshly fabricated. In this study, Li^+ form was examined for all experiments. Electroless plating was carried out to deposit platinum on both surfaces of a pure Nafion film. To clean the surfaces of the film, the film was immersed in a beaker of a boiling water/nitric acid (1/2) mixture for 30 min. This process also removed organic contaminants in the material. Then, the film was washed with water and boiled in water for 30 min. This process ensured complete hydration. Then, the film was soaked in a 0.01 M tetraamineplatinum(II) chloride solution at 25 °C for 2 h with agitation. The film was then rinsed with water and transferred to freshly prepared 0.01 M sodium borohydride at 25 °C for 2 h. Then, the film was rinsed with water, immersed in 1 M nitric acid solution for 30 min, and boiled in water for 30 min. This plating process was repeated three times. The film was finally soaked in 0.1 M lithium hydroxide solution for 10 h and rinsed well with water so that the counter cations were exchanged to Li^+.

Water Uptake of IPMC with Humidity. To identify a possible relationship between water uptake and relative humidity, first, a piece of the IPMC actuator (3 × 20 mm) was dried at 100 °C in vacuum for 10 h and weighed (21.1 mg). Then, the film was suspended in an environment with 30% relative humidity (RH). The humidity was increased using water vapor, the film was allowed to equilibrate and then weighed, and the process was then repeated. A graph of percentage mass gain versus humidity was plotted from the data.

Evaluation of Dynamic Performance. We developed a quantitative static and dynamic performance evaluation system especially for chemical actuators such as IPMC actuators. Because the actuator undergoes a large bending motion, a CCD camera was employed to follow the displacement. The evaluation system was composed of a programmable power supply (HP model 6632B), data acquisition board (DAQ) (National Instruments Inc.), CCD camera, image processing board, and balance. The images from the camera were preprocessed through the image processing board. The waveform of the potential applied to the actuators was fully controlled by the software. Here, homemade software was developed in LabView (National Instruments Inc.). The programmable power supply was a monopolar system that was converted to a bipolar system. The delay of the bipolar switching was less than 5 ms, and this timing was carefully adjusted by the software. Both the current and the potential were monitored through the DAQ. The measurement of the displacement was performed in a humidity-controlled chamber. The length of the actuator was carefully set to 16 mm on the stage by clamping 2 mm of the 18-mm actuator. The displacement was evaluated horizontally at 12 mm from the root. The mechanical force of the actuators was monitored by a balance having a homemade attachment to the actuators. All of the experiments were conducted at 25 °C.

SCHEME 2

$$NaBH_4 + 4[Pt(NH_3)_4]^{2+} + 8OH^- \longrightarrow 4Pt^0 + 16NH_3 + NaBO_2 + 6H_2O$$

Results and Discussion

Preparation of the Actuator. The fabrication of IPMC-type actuators includes three basic stages: (a) ion exchange from H^+ to the metal complexes in the matrix of Nafion, (b) chemical reduction using ionic reductants (i.e., surface metallization can be done if the reducing agent is negatively charged for a static repulsive inhibition of the reaction in the film), and (c) ion exchange to the final form.[5,32,33] In the first process, Nafion film was soaked in $[Pt(NH_3)_4]^{2+}$ solution to allow this platinum salt diffused into the film. Then, the film was transferred to a solution containing the anionic reduction agent BH_4^-. Scheme 2shows the primary reaction of the deposition of platinum. It is known that the penetration of the conductive layers onto Nafion results in dendritic branching and fractals.[33] After the metallization reaction, the film was finally soaked in lithium hydroxide solution to allow for the cation exchange of lithium and well washed and rinsed with water.

Actuator Performances. A square waveform of +2 and −2 V was applied to the actuator electrodes. The interval of each step was 20 s. As reported in many journal articles,[34] a bending motion toward the anode occurs as a result of an electric field. Here, it is known that the velocity of the actuation strongly depends on the species of cations such as Li^+, Na^+, K^+, Rb^+, Cs^+, and tetraalkylammonium cations.[34] The relaxation time in this work means the period during which the bending motion of the actuator is completely halted without manipulating the electric field. In fact, an interval time of 20 s might not be enough time to achieve full relaxation. In the strict sense of relaxation, it will take several hundreds of seconds to achieve full relaxation. To avoid unexpected deterioration of the electrode upon application of a potential for a long period, we limited this time to 20 s. During this time period, the relaxation bending process was clearly recorded.

As shown in Figure 1, the water uptake of IPMC was examined as a function of the relative humidity. Clearly, the film absorbs water effectively as a function of the humidity, and the maximum variation in the mass gain was ca. 22% at 98% RH. The tendency of the mass change of water uptake agrees with similar experimental results for Nafion membranes.[35] The average number of water molecules per sulfonic acid group at 0% RH has been reported to be 1.55.[35] In the humidity range of 0−50%, an additional water molecule was added to each sulfonic acid group. The ratio of H_2O/SO_3H was ca. 3−5. At higher humidities, this process becomes much more rapid, and water finally starts to condense on all regions of the membrane until the resulting pressure within its clusters is balanced by the elastic stresses that develop within the membrane. Nemat-Nasser et al. previously reported the relationship between

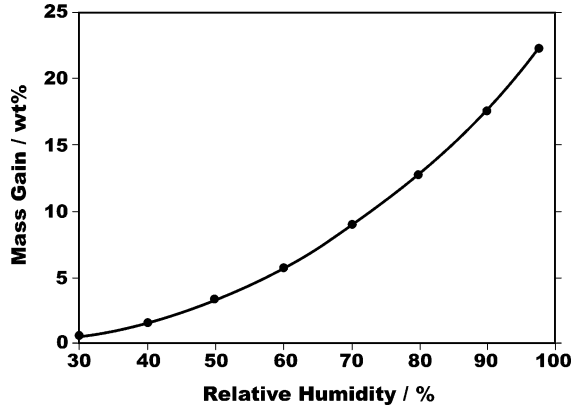

Figure 1. Percentage mass gain versus relative humidity for the actuator film.

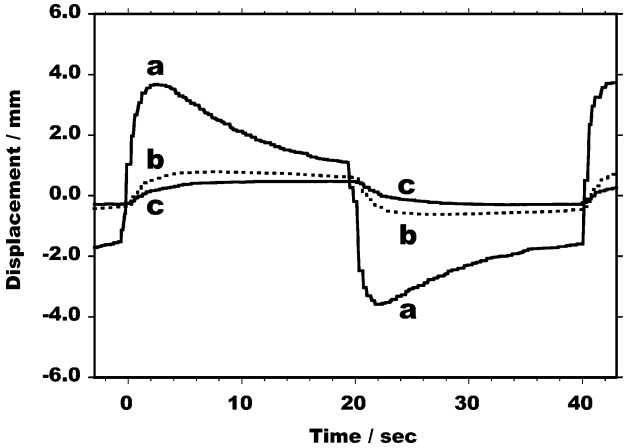

Figure 2. Displacement versus time profiles under various humidity conditions: (a) 90% (solid line), (b) 50% (dotted line), and (c) 30% (solid line).

hydration volume and stiffness as "stiffness is in inverse proportion to hydration volume".[36] That is, from the relation between the cross-sectional area and the hydration volume, the sample's cross-sectional area can be estimated at various hydration levels by simply measuring its weight. The mass of the sample can be calculated by the corresponding hydration volume and then the cross-sectional area. These results gave the stiffness as a function of hydration volume. Because there is no information on any relation between the hydration volume and the hydration state, however, it is difficult to correlate hydration state to stiffness quantitatively. Thus, our discussion here was to point out that the stiffness can be decreased if the hydration (state) is enhanced by humidity, because the increase in hydration volume is directly based on the absorption of water.

Figure 2 shows the displacement under various RH conditions of 90% (water uptake ca. 18%, solid line, curve a), 50% (ca. 3%, dotted line, curve b), and 30% (ca. 1%, solid line, curve c) obtained by applying a potential. Clearly, the displacement strongly depends on the humidity (water uptake), and curve a shows the largest displacement of ca. ±3.5 mm. This value is nearly 10 times larger than the ±0.3 mm value for curve c at 30% RH. The result agrees with the finding that the displacement depends on the level of hydration.[36] Here, the nature of the transport of water and hydrated ions within the IPMC film affects the moduli at different frequencies.[33] Thus, the effect of the humidity on the stiffness[34] (modulus of elasticity) should be an important factor in facilitating the bending motion and back-relaxation. We will discuss this behavior further below.

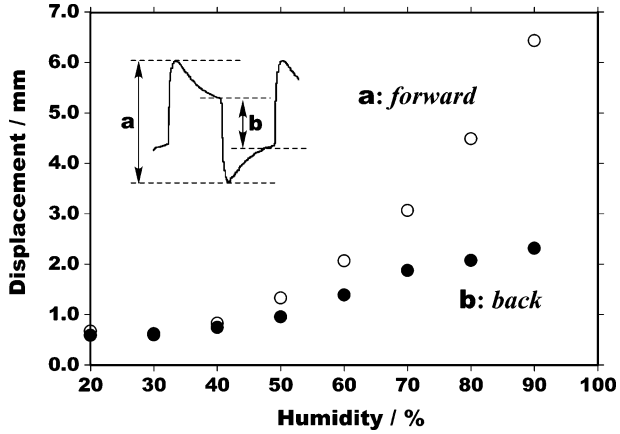

Figure 3. Maximum forward and backward displacements versus humidity, showing (a) each gap of the forward displacement (open symbols) and (b) each gap of the backward displacement (solid symbols).

Figure 2a clearly shows that the actuator exhibits a dramatic backward motion (i.e., a back-relaxation process[34,36]) just after the maximum forward displacement. This subsequent reverse motion is dramatically suppressed by decreasing the humidity. The theoretical and experimental frameworks have been discussed for several models of the mechanism of IPMC actuation.[22,34,36,37] Hydraulic models of IPMC actuation are important to understand this reverse mechanism. That is, when the potential is applied, the voltages cause the migration of ions (i.e., cations redistribute and migrate toward the cathode), and the hydraulic effect is assigned to the motion of water molecules that are contributing ions by solvation. As seen in Scheme 1, because Nafion has a hydrophobic backbone of fluorocarbon polymer that is separated from the hydrophilic clusters containing unbound solvated cations and fixed sulfonate groups, water redistribution affects the cluster volume and distribution of cations. These changes also impact the stiffness of the film. The stiffness is inversely proportional to the hydration volume,[34] that is, an increase in water uptake leads to a decrease in the stiffness. The secondary hydraulic effect involves electro-osmotic effects that are derived from the initial migration of ions.[36] After the migration of both cations and water toward the cathode, subsequent redistribution and reconfiguration of those species can be promoted by a slow buildup of a voltage and electro-osmotic effects.[36,38] The back-relaxation comes from the rearrangement of small mobile molecules.[36] From these findings, the slow diffusion of water into the elastically softened anode and out of the stiffened cathode can be considered to give the slow reverse relaxation.

The dependences of the maximum gaps of the forward displacement (a, open circles) and the backward displacement (b, solid symbols) on RH are shown in Figure 3. Both the forward and reverse displacements are increased by RH, primarily because of a decrease in the stiffness. Moreover, it is noted that the forward motion is strongly influenced by RH. Here, the two plots are very close when the RH is less than ca. 40%, and the reverse motion is eventually weakened.

Figure 4 shows the dependence of the charge on the humidity. Basically, the charge during the actuation is based on a compensation for migration of cations, faradic process for the electrolysis of water, and/or unexpected redox reactions of the electrode. A potential of 2 V is being applied to the electrodes in the experiment, and this potential is more than the value of ca. 1.23 V that is the theoretical potential for water electrolysis. Thus, except for unexpected degradation, both compensation

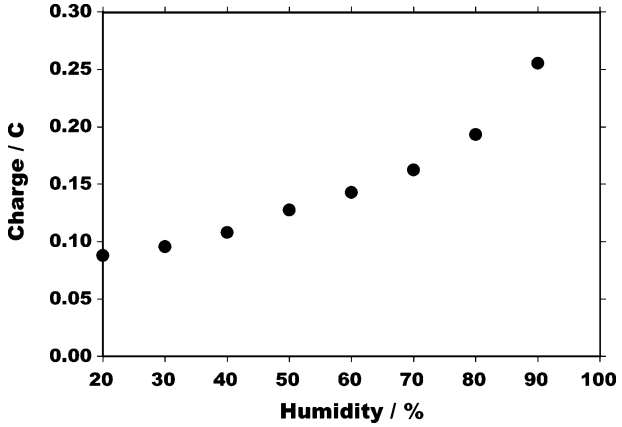

Figure 4. Dependence of charge on humidity.

of ions and electrolysis of water are expected to be a primary source of the charge. The charge would also depend on the mobility of the ions, the level of hydration, and the form of the cations. Given that the charge of ca. 0.25C near 90% RH is about 3 times higher than the charge of 0.09C near 20% RH, the increase in the charge is mainly due to the higher mobility of the hydrated cations and the electrolysis of water. Regarding the electrolysis of water, even if all of the 0.25C were being used for the electrolysis, the loss of water is estimated to be only 0.05 mg. Thus, this amount of water can easily be supplied under 90% RH conditions, so that the actuator can repeat the bending motion continuously at 2 V.

The velocities of both the forward and backward displacements are proportional to the humidity (Figure 5). Note that the velocities in Figure 5A are based on average velocities during forward and backward displacements, and the velocities in Figure 5B are based on the maximum differential velocities for forward and backward displacement. As can be seen in Figure 5B, the maximum forward velocity is ca. 14 mm/s, and this velocity is about 10 times faster than the backward displacement of 1.3 mm/s. The stiffness of the film is decreased by water uptake, but the diffusion of cations can be facilitated.[34] Therefore, as shown in Figure 5, an increase in water uptake results in an enhancement of the velocity of the displacement.

Figure 6 shows the time course of the displacement as the RH is changed from ca. 30% to ca. 90%. The displacement at 90% RH is about 10 times larger than the displacement at 40% RH. Note that a back-relaxation can be gradually observed with increasing RH above 50%. Above ca. 60% RH, the IPMC actuator shows a remarkable backward displacement that is nearly one-half of the maximum displacement. Figure 7A and 7B shows the time course of the force as a function of humidity, and a back-relaxation behavior can be recognized in the force generation. The maximum peak forces are 1 and 3 mN at 50% and 90% RH, respectively. This finding indicates that the hydration impacts an internal stress (i.e., modulus) of the film and this stress affects both the displacement (i.e., without loading) and the force (i.e., with loading). In the time course of the force generation, three patterns of profiles without relaxation (a), in transient (b), and with relaxation (c) can be seen in Figure 7A. Note that each scale is not the same in the comparison. The transient is located near ca. 50% RH. A similar transient can also be recognized in the displacement in Figure 6 at ca. 50% RH. Both the displacement and the force are enhanced by an increase in the humidity. Thus, the force can be increased if the displacement is increased. A highly hydrated actuator gives a larger bending displacement because of a decrease in the

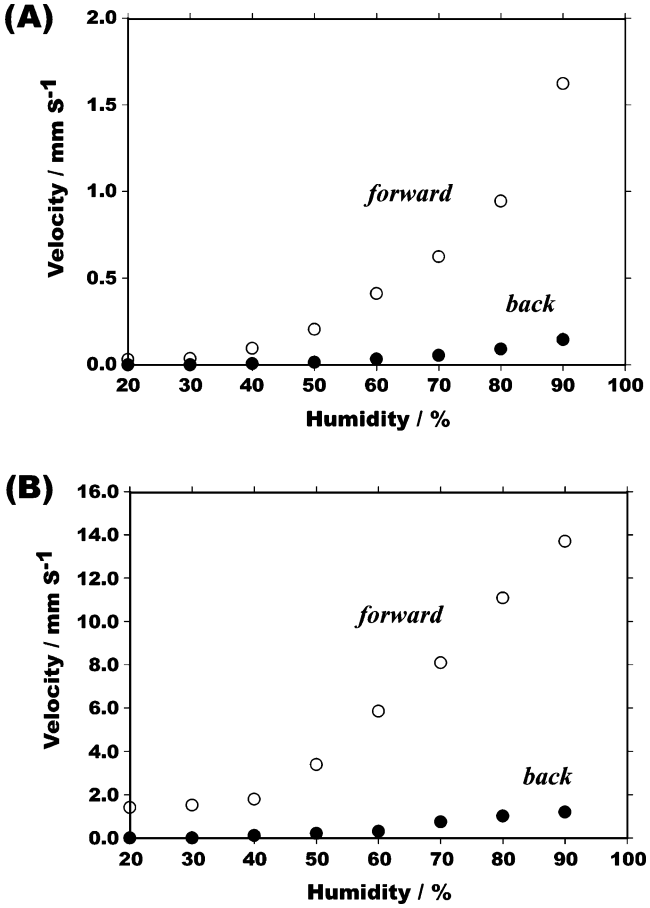

Figure 5. Velocity versus humidity for both forward and backward motion during actuation. The velocity was evaluated as (a) the average of the forward and backward displacements and (b) the maximum velocity of the forward and backward displacements.

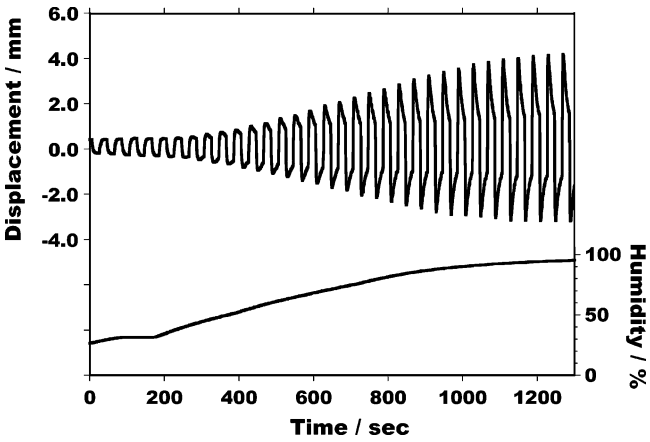

Figure 6. Displacement versus time under a ±2 V square waveform. The interval of each step is 20 s. The humidity was controlled from ca. 30% to ca. 90%.

stiffness and much more water transport. After the larger bending motion, a dramatic backward motion is seen clearly.

The stiffness of the film, the hydration state of the film (for both Nafion and mobile ions), and the hydration volume are affected by humidity. Thus, the relaxation process should be influenced by at least these parameters and should be intricate. If the humidity is increased, however, the relaxation time would be decreased as a result of a decrease in the stiffness, giving a smooth bending motion of the film. By compiling the results of the displacement and force profiles, the bending phenomena are revealed to be a result of internal stress of the film (or vice

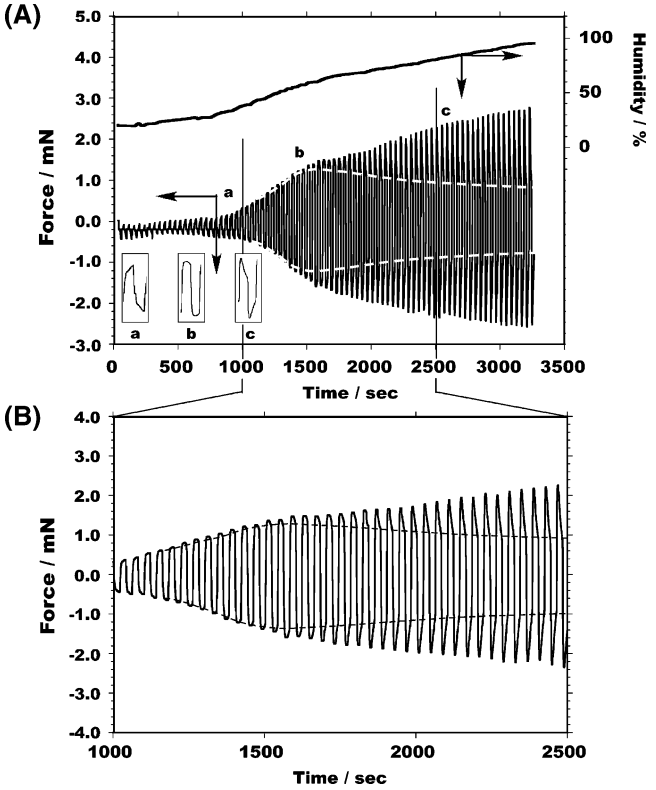

Figure 7. Force versus time and humidity under the ±2 V square waveform shown in Figure 1. The humidity was controlled from ca. 30% to ca. 90%. Three types of profiles (a−c) are shown. The time region of a from 1000 to 2500 s is expanded to b. In both plots a and b, the force after 20 s at each cycle is evaluated as a net force, and the net force is indicated by the supported dotted lines.

versa). Here, because a reaction to the stress necessitates a deformation of the film, both the displacement and the force generation would lead to a back-relaxation. In terms of an evaluation of the durability performance of the actuators, we focused on a metastable force during the back-relaxation process. In comparison to a quick forward displacement within seconds, this relaxation approaching a metastable state required tens or even hundreds of seconds.[36] To elucidate the metastable state, supported dotted lines were added to Figure 6A and 6B to indicate the force after 20 s at each cycle. As can be seen, the maximum plateau exists near 50% RH.

Force profiles a−c in Figure 7A are enlarged and presented in Figure 8with charging profiles at each cycle. Figure 8A−C corresponds to force profiles around 80%, 50%, and 30% RH, respectively. The maximum force and back-relaxation processes during force generation are very sensitive to the humidity. Under lower-humidity conditions (for example, ca. <50%), the actuator becomes "rigid", and the total displacement (i.e., bending performance) gets smaller. Under higher-humidity conditions (ca. >50%), the actuator becomes "soft", and the total displacement increases. Thus, the production of the force naturally relates to a balance of the rigidness and the bending performance of the film. One question might arise as to whether a larger force could be produced by an actuator that is rigid and has smaller bending capability or by an actuator that is soft and has a larger bending capability. In the comparison of experimental data in Figure 8A and 8C, a capability giving larger displacement is of primary importance in obtaining a larger force. In the charging profiles in Figure 8, the charge is balanced by the force generation and the humidity. During the force production consuming 0.15 C near 90% RH in Figure 7A, the charge is continuously consumed without any inflection points

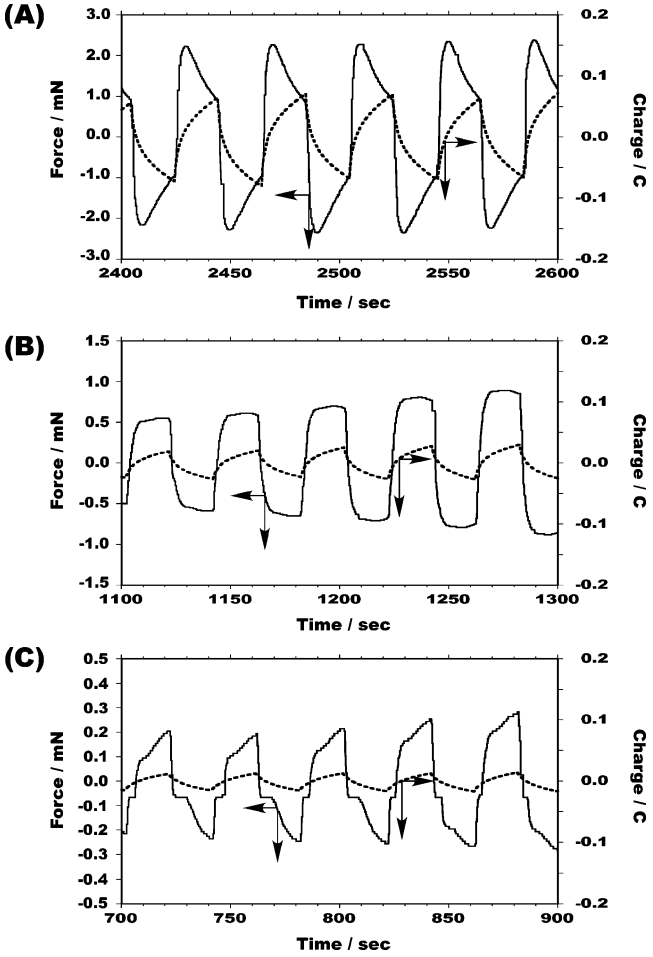

Figure 8. Force versus time and humidity. Data in Figure 8 are partially enlarged and shown at humidity values of (a) 80%, (b) 50%, and (c) 30%.

during the relaxation process. Here, the charge consumption can basically be understood as an accumulation of charge compensation for counterions, electrolysis of water, unexpected stray currents through the film, or platinum-related redox processes in the film. As long as charge compensation is for the migration of ions by the electric field conditions, having no clear inflection point on the charging process during back-relaxation suggests that the back-relaxation process might involve not the charge redistribution of ions but, rather, water redistribution. The experimental finding here would relate to water redistribution based on osmotic pressure and stiffness/hydration effects.[34,36]

We have evaluated continuous force generation by scanning the potential at 50 mV/s from 0 to 3.5 V. Before this experiment, we confirmed that potentials above 4 V were too high and caused serious damage to the actuator. Thus, the potential was limited to 3.5 V. Figure 9A shows the profile of the force under 40% RH, for which the maximum force is 2.6 mN at 3.5 V. Figure 9A also shows a long-period back-relaxation giving a negative force after open circuit. This negative force would come from an accumulated internal stress (as a modulus) during continuous force production. We are currently carefully focusing on this process, and the results will be reported elsewhere. The same experiments as depicted in Figure 9A were repeated under various RH values, giving the results shown in Figure 9B. Interestingly, Figure 9B demonstrates that the actuator can produce a maximum force of ca. 3.7 mN near 50% RH. Again, this would be a result of a balance of the rigidity and bending capability of the film. This finding clearly suggests that the

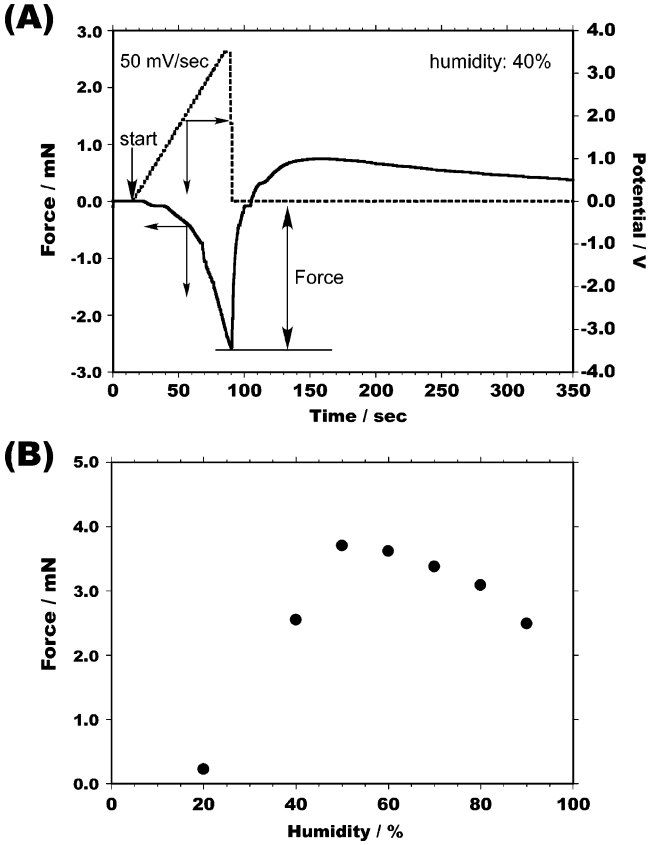

Figure 9. Force measurement of a Nafion−Pt-based actuator at 40% RH. The potential was scanned from 0 to 3.5 V at 50 mV/s. (A) The maximum force was evaluated at 3.5 V, and then the potential was set to 0 V to record a negative force generation. (B) Dependence of the force at 3.5 V on the humidity. The experimental procedure was the same as for A, and the force was evaluated at various humidities.

humidity (water uptake) has to be carefully considered to obtain the maximum performance of IPMC-type actuators.

Conclusion

Both forward and reverse displacements were dramatically enhanced by humidity. For instance, the forward displacement at 90% RH was nearly 10 times larger than the displacement at 30% RH. The primary reason for this observation is a decrease in stiffness resulting from water uptake. Here, water molecules were added to each sulfonate group, and at higher humidities, all regions of the membrane were condensed by water until the resulting pressure within its clusters was balanced. The hydraulic effect involves electro-osmotic effects that are derived from the migration of ions. These events enhance the velocity of the displacement and also promote a reverse relaxation process. The reverse relaxation process does not involve a major redistribution of counter cations. A reverse relaxation was also recognized during force generation, and this relaxation was dramatically sensitive to the humidity. During continuous force loading, the accumulated internal stress in the film gives a negative force. These results are consistent with the view that the bending phenomena are a result of the balance of internal stress and water transport in the film.

Acknowledgment. This work was partially supported by research grants from the University of Fukui.

References and Notes

(1) Osada, Y.; Gong, J. *Prog. Polym. Sci.* **1993**, (18), 187.

(2) Eichenbaum, G. M.; Kiser, P. F.; Simon, S. A.; Needham, D. *Macromolecules* **1998**, *31*, 5084−5093.

(3) Tanaka, T.; Fillmore, D.; Sun, S. T.; Nishio, I.; Swislow, G.; Shah, A. *Phys. Rev. Lett.* **1980**, *45*, 1636−1639.

(4) Harmona, M. E.; Tangb, M.; Frank, C. W. *Polymer* **2003**, *44* (16), 4547−4556.

(5) Millet, P.; Pineri, M.; Durand, R. *J. Appl. Electrochem.* **1989**, *19*, 162−166.

(6) Sadeghipour, K.; Salomon, R.; Neogi, S. *Smart Mater. Struct.* **1992**, *1*, 172−179.

(7) Oguro, K.; Asaka, K.; Takenaka, H. In *Proceedings of the 4th International Symposium on Micro Machine and Human Science*; IEEE Press: Piscataway, NJ, 1993; p 39.

(8) Asaka, K.; Oguro, K.; Nishimura, Y.; Mizuhata, M.; Tanaka, H. *Polym. J.* **1995**, (27), 436−440.

(9) Shahinpoor, M.; Bar-Cohen, Y.; Simpson, J. O.; Smith, J. *Smart Mater. Struct.* **1998**, *7* (6), R15−R30.

(10) Onishi, K.; Sewa, S.; Asaka, K.; Fujiwara, N.; Oguro, K. *Electrochim. Acta* **2001**, *46* (8), 1233−1241.

(11) Kim, K. J.; Shahinpoor, M. *Polymer* **2002**, *43*, 797−802.

(12) Noh, T.-G.; Tak, Y.; Nam, J.-D.; Choi, H. *Electrochim. Acta* **2002**, *47*, 2341−2346.

(13) Jung, K.; Nam, J.; Choi, H. *Sens. Actuators A* **2003**, *107*, 183−192.

(14) Baughman, R. H. *Synth. Met.* **1996**, *78* (3), 339−353.

(15) Mazzoldi, A.; Santa, A. D.; Rossi, D. D. In *Polymer Sensors and Actuators*; Osada, Y., De Rossi, D. E., Eds.; Springer-Verlag: Heidelberg, Germany, 1999.

(16) Kaneko, M.; Fukui, M.; Takashima, W.; Kaneto, K. *Synth. Met.* **1997**, *84*, 795−796.

(17) Madden, J. D.; Cush, R. A.; Kanigan, T. S.; Brenan, C. J.; Hunter, I. W. *Synth. Met.* **1999**, *105*, 61−64.

(18) Kawano, Y.; Wang, Y.; Palmer, R. A.; Aubuchon, S. R. *Polim.: Cienc. Tecnol.* **2002**, *12* (2), 96−101.

(19) Shahinpoor, M.; Kim, K. J. *Smart Mater. Struct. Int. J.* **2005**, *14* (1), 197−214.

(20) Heitner-Wirguin, C.; Bauminger, E. R.; A., L.; Kanter, F. B.; Ofer, S. *Polymer* **1980**, *21*, 1327−1329.

(21) Hsu, W. Y.; Timothy, T. D.; Gierke, D. *Macromolecules* **1982**, *15*, 101−105.

(22) Enikov, E. T.; Seo, G. S. *Sens. Actuators A* **2005**, *122*, 264−272.

(23) Lee, J. H.; Lee, J. H.; Nam, J.-D.; Choi, H.; Jung, K.; Jeon, J. W.; Lee, Y. K.; Kim, K. J.; Tak, Y. *Sens. Actuators A* **2005**, *118*, 98−106.

(24) Shahinpoor, M. In *Proceedings of the SPIE Conference on Smart Structures and Materials*; SPIE Press: Bellingham, WA, 1993; Vol. 1916, pp 40−50.

(25) Shahinpoor, M. In *Proceedings of SPIE Conferences on Electroactive Polymer Actuators and Devices*; SPIE Press: Bellingham, WA, 1999; Vol. 3669, pp 109−121.

(26) Kanno, R.; Kurata, A.; Hattori, M.; Tadokoro, S.; Takamori, T. In *Proceedings of the Japan−U.S.A. Symposium on Flexible Automation*; ISCIE/ASME: New York, 1994; Vol. 2, pp 691−698.

(27) Kanno, R.; Tadokoro, S.; Takamori, T.; Hattori, M. In *Proceedings of the IEEE International Conference on Robotics and Automation*; IEEE Press: Piscataway, NJ, 1996; Vol. 1, pp 219−225.

(28) Bao, X.; Bar-Cohen, Y.; Lih, S. In *Proceedings of the SPIE Smart Structures and Materials Symposium*; SPIE Press: Bellingham, WA, 2002; pp 4695−4727.

(29) Nemat-Nasser, S.; Li, J. Y. *J. Appl. Phys.* **2000**, *87* (7), 3321−3331.

(30) Shahinpoor, M.; Kim, K. J. *Smart Mater. Struct.* **2004**, *13* (6), 1362−1388.

(31) Kucernak, A. R.; Muir, B. *Electrochim. Acta* **2001**, *46*, 1313−1322.

(32) Takenaka, H.; Torikai, E.; Kawami, Y.; Wakabayashi, N. *Int. J. Hydrogen Energy* **1982**, *7*, 397−403.

(33) Shahinpoor, M. *Electrochim. Acta* **2003**, *48* (14−16), 2343−2353.

(34) Nemat-Nasser, S.; Wu, Y. *J. Appl. Phys.* **2003**, *93* (9), 5255−5267.

(35) James, P. J.; Elliott, J. A.; McMaster, T. J.; Newton, J. M.; Elliott, A. M. S.; Miles, M. J.; Hanna, S. *J. Mater. Sci.* **2000**, *35*, 5111−5119.

(36) Nemat-Nasser, S. *J. Appl. Phys.* **2002**, *92* (5), 2899−2915.

(37) Shahinpoor, M. *Electrochim. Acta* **2003**, *48* (14−16), 2343−2353.

(38) Bar-Cohen, Y. *Electroactive Polymer (EAP) Actuators as Artificial Muscles*; SPIE Press, 2001.